



# Forecasting Research

Forecasting Research Division  
Scientific Paper No. 30

**A shallow-water semi-geostrophic model on the sphere.**

by

**M.H. Mawson**

**January 1995**

**Meteorological Office  
London Road  
Bracknell  
Berkshire  
RG12 2SZ  
United Kingdom**

ORGS UKMO F

**National Meteorological Library**  
FitzRoy Road, Exeter, Devon. EX1 3PB



**Forecasting Research Division  
Scientific Paper No. 30**

**A shallow-water semi-geostrophic model on the sphere.**

**by**

**M.H. Mawson**

**January 1995**



# A shallow-water semi-geostrophic model on the sphere.

Mark H. Mawson

*Forecasting Research Division, Meteorological Office,  
London Road, Bracknell, Berkshire. RG12 2SZ.*

January 3, 1995

## Abstract

The  $f$ -plane semi-geostrophic equations have provided much insight into atmospheric motions and we wish to see if more can be gained by removing the  $f$ -plane restriction. As a first step we begin by considering the shallow-water semi-geostrophic equations on the sphere and describe a numerical solution procedure for them based on a semi-Lagrangian predictor/corrector method. It is demonstrated, numerically, that the method appears to converge to a true solution of the semi-geostrophic equations for fixed resolution, and this suggests that there exists a unique solution to the continuous equations. The results from several idealised and real data test problems are presented and show that the scheme is stable and accurate. The results are compared with those obtained from a shallow-water semi-Lagrangian primitive equation model. The simulations are broadly similar but the semi-geostrophic solution maintains stronger anticyclones than the primitive equation model. This is in agreement with results expected after considering  $f$ -plane baroclinic wave simulations with the effects of spherical geometry taken into account.

## 1 Introduction

In order to improve the current numerical weather prediction models it is essential to understand more about the real atmosphere and about numerical models of it. In particular, we need to understand how models react to physical forcing. To gain insight into how both the atmosphere and the models work much work has been done with simpler models of the atmosphere. These simpler models are usually based on equations which have had a further level of approximation made to them,



and in the early days of computers were used as the basis for providing weather predictions, see for example Charney, Fjortoft & von Neumann (1950). Much work has been done with simpler equations confined to a plane where the Coriolis force due to the Earth's rotation is assumed constant, known as the  $f$ -plane approximation. This approximation is valid for many phenomena of interest in mid-latitudes and much insight has been gained from running these models in this way. However only a restricted class of these models can be used in spherical geometry. The long term aim of the work is to try to gain more insight into numerical models by adding extra detail to that provided by quasi-geostrophic models whilst avoiding the complexity incurred by using a primitive equation model.

The equations studied in this paper are the semi-geostrophic equations, henceforth SG, first suggested by Eliassen (1948), the usefulness of which was first really seen in the work of Hoskins & Bretherton (1972). In their paper they demonstrated the ability of the equations forced by a deformation field to produce idealised atmospheric fronts which possessed many of the characteristics of real fronts. Since then these equations have been used extensively to investigate the role of moist processes in the formation of atmospheric weather fronts, see for example Holt (1990), Holt & Thorpe (1991), Castelli, Bras & Emanuel (1993). They have also been used to simulate idealised flow over a mountain (Cullen, Chynoweth & Purser 1987, Pierrehumbert 1985), where the topic of interest was the effect of a barrier on a uniform flow normal to it. This is of interest in the simulation of downslope wind storms where sudden strong winds and a significant rise in temperature can occur; such storms are common in mountainous areas such as the Rockies. The equations have also been used to look at non-linear baroclinic waves (Snyder, Skamarock & Rotunno 1991, Whitaker 1993, Davies, Schar & Wernli 1991) and the results compared with primitive equation, henceforth PE, solutions. The equations, including friction, have also been used to look at idealised sea breeze simulations, Cullen (1989*b*). Wu & Blumen (1982) have looked at the interaction between the semi-geostrophic equations and the atmospheric boundary layer as has Young (1973).

The semi-geostrophic equations on the sphere are defined by taking the basic definition of the equations following Hoskins (1975) and allowed the Coriolis pa-



parameter  $f$  to vary and included spherical geometry. The solution procedure for the  $f$ -plane SG equations adopted by previous authors depends on using a coordinate transformation to produce a simpler equation set in the new co-ordinates. This approach cannot be used with variable  $f$  and in this paper we describe a numerical method for solving the equations without recourse to a co-ordinate transformation. The semi-geostrophic equations on the sphere do not conserve, in a Lagrangian sense,  $\zeta_g \cdot \nabla \theta$  in three dimensions with  $\zeta_g$  defined as in Hoskins, or  $\zeta_g/h$  in the shallow-water case where

$$f\zeta_g = \left[ f + \frac{1}{a \cos \phi} \frac{\partial v_g}{\partial \lambda} + \frac{u_g \tan \phi}{a} \right] \left[ f - \frac{1}{a} \frac{\partial u_g}{\partial \phi} \right] + \left[ \frac{1}{a} \frac{\partial v_g}{\partial \phi} \right] \left[ \frac{1}{a \cos \phi} \frac{\partial u_g}{\partial \lambda} - \frac{v_g \tan \phi}{a} \right] \quad (1)$$

$\zeta_g$  can be considered to be the semi-geostrophic absolute vorticity. To try and retain such properties for varying  $f$  both Shutts (1989) and Salmon (1985) have used a Hamiltonian approach to the geostrophic momentum approximation but derived different systems of equations. The equations derived by Salmon conserve  $f\zeta_g$  in a Lagrangian sense in his dual space. Shutts's approach was to obtain equations valid on the sphere which also conserved energy and the semi-geostrophic potential vorticity. The equations he derives, called the *planetary semi-geostrophic* equations, differ from the semi-geostrophic equations of Hoskins in that the Lagrangian derivative term in the meridional momentum equation becomes

$$\sin \phi \frac{D}{Dt} (v_g \sin \phi)$$

These equations allow non-zero height gradients along the equator unlike the semi-geostrophic equations, and hence support a wider class of solutions there. It is an open question as to which of the three versions of the semi-geostrophic equations for variable  $f$  is the most useful one to investigate atmospheric motions on the sphere. Those derived from a Hamiltonian approach have the advantage that they preserve some of the properties of the full equations which the semi-geostrophic equations do not. The numerical method described herein is for the semi-geostrophic equations on the sphere since it is these we have chosen to study. In principle this method could be applied to the planetary semi-geostrophic equations, but care would have



to be exercised at the equator where  $v_g$  is allowed to be infinite but is multiplied by  $\sin\phi$  which is zero.

Definitions of balance other than geostrophic can be used to define more general equation sets, such as the *linear balance equations* and the *balance equations* described in McWilliams & Gent (1980). Discussion of these equations, along with other balanced equations, can be found in that paper and in others by the same authors (Gent & McWilliams 1983*a*, Gent & McWilliams 1983*b*) and more recently in Allen, Barth & Newberger (1990). These models are more general than those derived from geostrophic balance but because they describe more types of atmospheric motion they may be less useful in providing the understanding that we seek. This is because their extra complexity may make it more difficult to isolate the important processes. The logical approach seems to be to extract all the understanding we can from each level of simple model and to gradually increase the models' complexity as our understanding grows. It is thus advisable that we discover what we can from models based on geostrophic balance before embarking on more complex systems.

We adopt a typical approach when embarking on looking at a three-dimensional problem on the sphere, and that is to first consider the shallow-water form of the equations. Instead of the full 3-d problem there is only a 2-d problem to be solved with the variation in the third direction being represented only by the changing height of the free surface. It has often been found that the major problems in implementing a numerical method for a 3-d model can be found in the equivalent shallow-water problem, such as problems with the co-ordinate poles. Methods which work for the shallow-water problem are often readily generalised to the full 3-d one with little extra effort. In the rest of this paper a semi-Lagrangian predictor/corrector numerical method for solving the shallow-water semi-geostrophic equations on the sphere is described. The method is used to integrate forward in time both idealised and real atmospheric initial data, and these simulations are compared with those from a shallow-water primitive equation model. The shallow-water simulations provide some insight into the underlying behaviour of the 3-dimensional equations but it is not expected that they will provide any significant new insight into the behaviour of the real atmosphere. The extra understanding we are looking for, it is



hoped, will be provided by the full 3-dimensional model. The extension of this work to 3-dimensions on the sphere is outside the scope of this paper.



## 2 Solution procedure

The shallow-water SG equations in spherical polar co-ordinates  $(\lambda, \phi)$  are

$$\frac{\partial h}{\partial t} + \nabla \cdot (h \underline{u}) = 0 \quad (2)$$

$$\frac{D \underline{u}_g}{Dt} = -g \nabla h - f \underline{k} \times \underline{u} \quad (3)$$

$$\frac{g}{a \cos \phi} \frac{\partial h}{\partial \lambda} - f v_g = 0 \quad (4)$$

$$\frac{g}{a} \frac{\partial h}{\partial \phi} + f u_g = 0 \quad (5)$$

where  $f = 2\Omega \sin \phi$ ,  $a$  is the radius of the sphere,  $g$  is the gravitational acceleration,  $h$  is the height of the free surface,  $\underline{u}_g = (u_g, v_g)$  is the geostrophic wind field and  $\underline{u} = (u, v)$  is the full wind field. We refer to equation (2) as the *mass* or *continuity* equation, equation (3) as the *momentum* equation and equations (4) and (5) as the *balance* equations. Before constructing a numerical procedure to solve this system of equations it would be advantageous to prove analytically under what conditions there exists a unique solution. Some progress towards this goal has been made, see Mawson (1994), but the result is as yet unproven. The approach adopted was to show that the system of equations (2)-(5) could be reduced to one second order variable coefficient partial differential equation for  $\partial h / \partial t$  away from the equator with boundary conditions of

$$\frac{\partial}{\partial \lambda} \left( \frac{\partial h}{\partial t} \right) = 0, \quad \frac{\partial}{\partial \phi} \left( \frac{\partial h}{\partial t} \right) = 0$$

at the equator. The condition for the partial differential equation to be elliptic is

$$q > \frac{1}{4} (\nabla \cdot \underline{u}_g)^2 \quad (6)$$

where  $q = f \zeta_g$ . We note that on an  $f$ -plane this is simply  $q > 0$ , which is the existence condition for solutions of the semi-geostrophic equations in this case, see Cullen & Purser (1989). This constraint insists that no semi-geostrophic absolute vorticity of the wrong sign is present in either hemisphere. A recent idealised primitive equation study, Rodwell & Hoskins (1995), suggests that where potential vorticity of the wrong sign is advected across the equator rapid accelerations occur consistent with inertial instability and the potential vorticity is rapidly modified to be of the correct



sign. Any method used to enforce the constraint in the semi-geostrophic model can be considered as a parametrization of this effect. As yet we have been unable to prove that the partial differential equation defined in each hemisphere with the given equatorial boundary condition has a unique solution on the sphere. The analytic approach predicts just the height tendency and calculates the others from it via equations (2)-(5). The values calculated from the predicted  $h$  values are unique except at the equator, where the only equation which defines  $\underline{u}$  is the continuity equation, since  $\nabla h = 0$  and hence  $\underline{u}_g = 0$ . Thus only the divergent part of the full wind field is defined and the rotational part remains undefined. An alternative approach to solving the equations is to use a predictor/corrector method, where we discretize in time and try to prove existence and uniqueness for a fixed timestep, and then try to show the same results hold as the timestep tends to zero. The predictor/corrector method consists of fixing  $\underline{u}$  at time  $t$  and predicting  $h, \underline{u}_g$  at time  $t + \Delta t$ . The values obtained at  $t + \Delta t$  will, in general, not satisfy the balance equations (4)-(5) and they are used to form a correction equation which determines the corrections required to  $h$  and  $\underline{u}_g$  in terms of corrections to  $\underline{u}$ . The correction equation which we need to solve is a second order variable coefficient partial differential equation away from the equator and is elliptic provided that the same constraint as before, (6), is satisfied. Also as in the other approach, Neumann like boundary conditions are applied at the equator and the rotational part of the wind field correction at the equator is similarly undefined. This approach is similar to that adopted by Cullen (1989a) in his numerical model for the 2-dimensional  $(x, z)$   $f$ -plane version of the SG equations. This approach is less suited for analytic studies of the equations, but it is an open question as to which would be the best basis for a numerical scheme. In the rest of this section we describe the implementation of the predictor/corrector approach in a numerical model. Since the prediction part is straightforward and can be solved easily using either Eulerian or semi-Lagrangian schemes, we begin by considering the correction step after introducing the following notation and grid-staggering.



## 2.A Notation and Grid-Staggering.

Given an  $m \times n$  array of points equally spaced on the sphere we define the following notation for averaging and centred finite difference operators in spherical polar co-ordinates  $(\lambda, \phi)$  for a sphere of radius  $a$ .

$$\Delta\lambda = 2\pi/m, \quad \Delta\phi = \pi/(n-1)$$

$$\delta_\lambda h(\lambda, \phi) = \frac{1}{a\Delta\lambda \cos\phi} (h(\lambda + \Delta\lambda/2, \phi) - h(\lambda - \Delta\lambda/2, \phi))$$

$$\delta_\phi h(\lambda, \phi) = \frac{1}{a\Delta\phi} (h(\lambda, \phi + \Delta\phi/2) - h(\lambda, \phi - \Delta\phi/2))$$

$$\delta_{\phi c} h(\lambda, \phi) = \frac{1}{a\Delta\phi \cos\phi} (h(\lambda, \phi + \Delta\phi/2) \cos(\phi + \Delta\phi/2) - h(\lambda, \phi - \Delta\phi/2) \cos(\phi - \Delta\phi/2))$$

$$\overline{h(\lambda, \phi)}^\lambda = (h(\lambda + \Delta\lambda/2, \phi) + h(\lambda - \Delta\lambda/2, \phi))/2$$

$$\overline{h(\lambda, \phi)}^\phi = (h(\lambda, \phi + \Delta\phi/2) + h(\lambda, \phi - \Delta\phi/2))/2$$

We also define

$$\underline{U} = (U, V) = (uh, vh)$$

The grid used for in the model is shown in figure 1 and is based on a D-grid for the balanced wind variables and a C-grid for the other variables. The location of the geostrophic wind components is chosen so that when centred finite differences are applied to the corrector equation we have the smallest possible stencil, a five point star. This grid also has the advantage that no interpolation is required when centred finite-differences are applied to the pressure gradient terms in the advection equations. To calculate  $\partial h / \partial t$  at  $\phi = 0$  to satisfy the boundary conditions in the corrector step a height point is placed at the equator. A height point is also placed at the poles. For further discussion of grid choices see Mawson (1994).

## 2.B Correction Step

Assume that we have made a first estimate of the solution at time  $t + \Delta t$  using equations (2)-(3) given by values of  $\underline{u}_g$  and  $h$  which do not satisfy equations (4) and (5). Estimate a correction to the velocity field, denoted by  $\underline{U}^A$ , which is required so that the balance equations, (4) and (5), are satisfied. The corrections implied by



i	i+1/2	i+1	
$h$	$u, v_g$	$h$	j
$v, u_g$		$v, u_g$	j+1/2
$h$	$u, v_g$	$h$	j+1

Figure 1: SG model grid staggering.

this velocity field are given by equations (2) and (3) but using  $\underline{U} + \underline{U}^A$  instead of  $\underline{U}$  as the advecting velocity giving

$$\frac{\Delta h}{\Delta t} = -(\delta_\lambda U^A + \delta_{\phi c} V^A) \quad (7)$$

$$\frac{\Delta u_g}{\Delta t} = -\left(\overline{\left(\frac{U^A}{\bar{h}^\lambda}\right)^\phi}^\lambda \delta_\lambda u_g\right) - \frac{V^A}{\bar{h}^\phi} \delta_{2\phi} u_g + \left(\frac{U^A}{\bar{h}^\lambda} v_g\right)^{\lambda\phi} \frac{\tan\phi}{a} + \frac{fV^A}{\bar{h}^\phi} \quad (8)$$

$$\frac{\Delta v_g}{\Delta t} = -\frac{U^A}{\bar{h}^\lambda} \delta_{2\lambda} v_g - \left(\overline{\left(\frac{V^A}{\bar{h}^\phi}\right)^\lambda}^\phi \delta_\phi v_g\right) - \frac{U^A}{\bar{h}^\lambda} \bar{u}_g^{\lambda\phi} \frac{\tan\phi}{a} - \frac{fU^A}{\bar{h}^\lambda} \quad (9)$$

where  $\Delta$  represents the difference between the solution which satisfies the balance equations at the new time level and the predicted values. In equations (8) and (9) the advection terms for the corrections are approximated by a simple forward Euler scheme. A more complicated scheme can be chosen but at the penalty of obtaining a more complicated correction equation. Substituting  $h + \Delta h$  and  $\underline{u}_g + \Delta \underline{u}_g$  into equations (4) and (5) gives the following corrector equations,

$$g\delta_\lambda \Delta h - f\Delta v_g = -R_{ew} \quad (10)$$

$$g\delta_\phi \Delta h + f\Delta u_g = -R_{ns} \quad (11)$$

where  $R_{ew}$  and  $R_{ns}$  are the residuals of equations (4) and (5) for the predicted values. Substituting for the corrections  $\Delta h$  and  $\Delta \underline{u}_g$  from equations (7)–(9) into



equations (10) and (11) and noting that  $\Delta h = -\Delta t D$  where  $D = \nabla \cdot \underline{U}$  we obtain

$$g\delta_\lambda D - f \left[ f + \frac{1}{\bar{h}^\lambda} \delta_{2\lambda} v_g + \frac{1}{\bar{h}^\lambda} \bar{u}_g^{\lambda\phi} \frac{\tan\phi}{a} \right] U^A - f \left( \overline{\left( \frac{V^A}{\bar{h}^\phi} \right)^\lambda} \delta_\phi v_g \right)^\phi = \frac{R_{ew}}{\Delta t} \quad (12)$$

$$g\delta_\phi D + f \left[ \left( \overline{\left( \frac{U^A}{\bar{h}^\lambda} \right)^\phi} \delta_\lambda u_g \right)^\lambda - \left( \frac{U^A}{\bar{h}^\lambda} v_g \right)^{\lambda\phi} \frac{\tan\phi}{a} \right] - f \left[ f - \frac{1}{\bar{h}^\phi} \delta_{2\phi} u_g \right] V^A = \frac{R_{ns}}{\Delta t} \quad (13)$$

It is now possible to substitute for  $V^A$  in equation (12) using equation (13) and for  $U^A$  in equation (13) from equation (12) provided that the terms multiplying them are non-zero. However because of the averaging incurred by using the staggered grid this would cause the equations at any point to be coupled to the equations at all other points. This coupling introduced by our grid staggering can be avoided by defining an iterative method for solving the equation which evaluates the terms which cause the coupling using the solution obtained at the previous iteration. Denoting the  $i$ th iterate by superscript  $i$  and evaluating the terms which imply the coupling at iteration  $i - 1$  gives

$$gA\delta_\lambda D^i - U^{A^i} - Af \left( \overline{\left( \frac{V^{A^{i-1}}}{\bar{h}^\phi} \right)^\lambda} \delta_\phi v_g \right)^\phi = \frac{AR_{ew}}{\Delta t} \quad (14)$$

$$gB\delta_\phi D^i - V^{A^i} + Bf \left[ \left( \overline{\left( \frac{U^{A^{i-1}}}{\bar{h}^\lambda} \right)^\phi} \delta_\lambda u_g \right)^\lambda - \left( \frac{U^{A^{i-1}}}{\bar{h}^\lambda} v_g \right)^{\lambda\phi} \frac{\tan\phi}{a} \right] = \frac{BR_{ns}}{\Delta t} \quad (15)$$

with

$$A = \frac{1}{f \left[ f + \frac{1}{\bar{h}^\lambda} \delta_{2\lambda} v_g + \frac{1}{\bar{h}^\lambda} \bar{u}_g^{\lambda\phi} \frac{\tan\phi}{a} \right]}$$

$$B = \frac{1}{f \left[ f - \frac{1}{\bar{h}^\phi} \delta_{2\phi} u_g \right]}$$

Taking the divergence of equations (14) and (15) gives, away from the equator,

$$\begin{aligned} \delta_\lambda (gA\delta_\lambda D^i) + \delta_{\phi c} (gB\delta_\phi D^i) - D^i &= \delta_\lambda \left( \frac{AR_{ew}}{\Delta t} \right) + \delta_{\phi c} \left( \frac{BR_{ns}}{\Delta t} \right) \\ &+ \delta_\lambda \left( Af \left( \overline{\left( \frac{V^{A^{i-1}}}{\bar{h}^\phi} \right)^\lambda} \delta_\phi v_g \right)^\phi \right) \\ &+ \delta_{\phi c} \left( Bf \left[ \left( \overline{\left( \frac{U^{A^{i-1}}}{\bar{h}^\lambda} \right)^\phi} \delta_\lambda u_g \right)^\lambda - \left( \frac{U^{A^{i-1}}}{\bar{h}^\lambda} v_g \right)^{\lambda\phi} \frac{\tan\phi}{a} \right] \right) \end{aligned} \quad (16)$$



Setting  $\underline{U}^{A^0} = 0$  and stopping the iterative procedure after just one iteration is equivalent to omitting the terms which imply the coupling. This simplification is similar to omitting a term in the SIMPLEC algorithm for solving the Navier-Stokes equations which leads to a simpler scheme at the expense of iterating the complete correction step, see Van & Raithby (1984) and Wen & Ingham (1993). The condition for equation (16) to have a unique solution, ie be elliptic, is the discrete version of equation (6). However on each iteration we only require that  $A$  and  $B$  are of the same sign and this is true if the data is inertially stable in the co-ordinate directions, since then they are both positive. However it is important to note that for the iterative procedure to converge to the correct solution the full ellipticity condition, inertial stability in all directions, must hold. To solve the correction problem on the sphere we now need to form the correction equation at  $\phi = 0$ , the equator, since the derivation of equation (16) assumes  $f \neq 0$ . At  $\phi = 0$  because of our choice of grid-staggering we only have equation (10) since equation (11) is defined half a grid-length polewards of the equator where  $f \neq 0$ . Hence at the equator the correction equation is

$$\Delta t \delta_\lambda D = R_{ew} \quad (17)$$

In the continuous problem there are two equations to be satisfied at  $\phi = 0$  and these form Neumann like boundary conditions for the partial differential equation. An alternative to enforcing the Neumann like boundary condition at the equator is to use a Dirichlet condition. This is only possible if the solution at the equator can be found before solving for the rest of the domain. Equation (17) is easily solved to give

$$D = e(\lambda) + s(\phi)$$

where  $e(\lambda)$  is the solution of equation (17) and  $s(\phi)$  is some arbitrary function. A similar result holds for the continuous problem. We note that  $s(\phi)$  is simply the zonal mean solution of equation (16), or the real Fourier coefficient  $a_0$  in a Fourier expansion of the solution  $D$  in the  $\lambda$ -direction given by

$$D(\lambda, \phi) = a_0(\phi) + \sum_{k=1}^{\infty} a_k(\phi) \cos(k\lambda) + ib_k(\phi) \sin(k\lambda)$$



We could now use this transform on equation (16) to find the coefficient  $a_0$ . A cheaper, although exactly equivalent, way is to integrate both sides of the equation with respect to  $\lambda$  over  $[0, 2\pi)$ . Doing this we obtain

$$\int_0^{2\pi} gB\delta_{\phi c}(\delta_{\phi}D)d\lambda - a_0 = \int_0^{2\pi} RHSd\lambda - \int_0^{2\pi} \delta_{\phi c}(gB\delta_{\phi}D)d\lambda$$

where we have dropped the iterative superscripts and noted that

$$\int_0^{2\pi} Dd\lambda = a_0$$

with the right hand side of equation (16) denoted by  $RHS$ . It is not possible to solve this equation exactly without knowing the solution over the domain excluding the equator. However an estimate of the Dirichlet boundary condition can be found if we assume that the second integral on the right hand side is negligible and approximate the one on the left hand side by

$$\delta_{\phi c}(\delta_{\phi}a_0) \int_0^{2\pi} gBd\lambda$$

we obtain

$$\delta_{\phi c}(\delta_{\phi}a_0) \int_0^{2\pi} gBd\lambda - a_0 = \int_0^{2\pi} RHSd\lambda$$

The solution of this is easily obtained since on the C-grid  $B$  is not evaluated at  $f = 0$  and hence does not become infinite. For the test problems performed in section 3 using this procedure to find  $a_0$  and then solving equation (16) with the approximate Dirichlet boundary condition and only one iteration did produce a noticeable unremoved residual at the equator on the first application of the corrector step on a timestep. However this residual was removed with one iteration of the corrector step. As we are unable to prove analytically that this procedure converges to the solution that would have been obtained by solving equation (16) to convergence with the correct boundary condition, either Neumann like or Dirichlet equivalent, we must rely on some numerical tests to satisfy ourselves that this is likely. These tests are discussed in section 2.F. Equation (16) with the Dirichlet boundary condition at the equator is solved via a multigrid method. Multigrid methods on the sphere are described in Barros (1991) and the implementation used here is similar to



that described therein, see Mawson (1994) for complete details. Having solved the equation (16) with  $i = 1$ , then  $U^A$  and  $V^A$  are found uniquely by substituting  $D$  in equations (14) and (15), with the exception that we cannot find  $U^A$  at the equator. This problem is overcome by noting that both  $D$  at the equator and  $V^A$  either side of the equator are well defined and

$$\delta_\lambda U^A = D - \delta_{\phi c} V^A$$

Solving this for  $U^A$  at  $\phi = 0$  given  $D$  and  $V^A$  does not give a unique solution as it introduces a constant of integration, in this case an arbitrary function of  $\phi$ . This arbitrary function represents the rotational part of  $U^A$  which we choose to set to zero. This corresponds to the fact that in the analytic method the rotational part of  $\underline{u}$  is undefined. The calculated values of  $D$  and  $\underline{v}^A$  are now used to calculate the corrections  $\Delta h$  and  $\Delta \underline{u}_g$  using equations (7) to (9). The value of  $\underline{U}$  at the new time level is given by  $\underline{U} + \underline{U}^A$ .

## 2.C Semi-Lagrangian Prediction Scheme

The mass equation written in Lagrangian form is

$$\frac{Dh}{Dt} = -h \nabla \cdot \underline{u}$$

and this can be discretized to second order accuracy in time via a semi-Lagrangian method by either

$$h_a = h_d - \Delta t (\nabla \cdot \underline{u}_d(t) + \nabla \cdot \underline{u}_a(t + \Delta t)) / 2$$

or

$$h_a = h_d - \Delta t \nabla \cdot \underline{u}_m(t + \Delta t / 2)$$

where subscript  $a$  denotes a value at the arrival point, subscript  $d$  a value at the departure point, and subscript  $m$  a value at the mid-point, of the trajectory. Since there is no predictive equation for  $\underline{u}$  the values at time levels greater than  $t$  in these equations could be calculated by extrapolation. The problem with using the semi-Lagrangian approach to solve this equation is that it introduces an inconsistency



between how the equation is solved in the predictor and corrector steps. This inconsistency can lead to large errors near the equator where only  $\nabla \cdot \underline{U}$  is well defined. To remove this inconsistency the flux form of the mass equation

$$h_a(t + \Delta t) = h_a(t) - \nabla \cdot \underline{U}_a(t)$$

is used and this is only first order accurate in time.

For momentum the vector approach of McDonald & Bates (1989), as described in Bates, Semazzi, Higgins & Barros (1990), is adopted and we refer the reader to these papers for details. We note that this approach does not suffer from any problems due to the polar singularity and any velocities required at the poles can be obtained by finding the local cartesian vector at the pole, see McDonald & Bates (1989). Writing the momentum equation in its vector form

$$\frac{D\underline{u}_g}{Dt} = -g\nabla h - f\underline{k} \times \underline{u}$$

where  $\underline{k}$  is the usual unit vector in the direction normal to the surface of the sphere, and discretizing to second order accuracy in time gives

$$\begin{aligned} \underline{u}_{g_a} = \underline{u}_{g_d} - \frac{\Delta t}{2} [(g\nabla h_d(t) + (f\underline{k} \times \underline{u}(t))_d) \\ + (g\nabla h_a(t + \Delta t) + (f\underline{k} \times \underline{u}(t + \Delta t))_a)] \end{aligned} \quad (18)$$

As already noted we do not have a value for  $\underline{U}$  at time levels greater than  $t$  and extrapolating  $U$  can lead to large errors for geostrophically balanced flows where the pressure gradient and coriolis terms should cancel. To minimise these errors only the values at time  $t$  are used since the flow is balanced at that time. We thus arrive at the first order accurate in time discretisation

$$\underline{u}_{g_a} = \underline{u}_{g_d} - \Delta t [g\nabla h_d(t) + (f\underline{k} \times \underline{u}(t))_d] \quad (19)$$

Implementing this discretisation leads to model runs failing in the region of the poles. The problem is the appearance of a very noisy  $q$  field containing many negative values which the procedure to enforce the ellipticity condition fails to remove adequately. The reason for their appearance in the solution can be found by looking at the derivation of the evolution equation for  $q$ . Near the poles  $\partial f / \partial \phi$  is approximately



zero and  $q$  should be almost conserved. To obtain this conservation the proof requires that

$$\frac{1}{a \cos \phi} \frac{\partial}{\partial \lambda} \left( \frac{g}{a} \frac{\partial h}{\partial \phi} \right) = \frac{1}{a \cos \phi} \frac{\partial}{\partial \phi} \left[ \cos \phi \left( \frac{g}{a \cos \phi} \frac{\partial h}{\partial \lambda} \right) \right]$$

where the terms in the  $()$  brackets are the pressure gradient terms evaluated in the predictor step. Using the discretisation of equation (19) this does not hold at the departure points since they may no longer be uniformly spaced due to both the evolution of the trajectories for the different points on the staggered grid and errors in calculating the trajectories. This conservation requirement can be satisfied by using the values at the arrival point at the old time-level which is still a first order accurate in time approximation given by

$$\underline{u}_{g_a} = \underline{u}_{g_d} - \Delta t [g \nabla h_a(t) + (f \underline{k} \times \underline{u}(t))_a] \quad (20)$$

Using this discretisation the model shows no signs of developing areas of noise or negative  $q$  near the poles. We note that in Bates, Li, Brandt, M<sup>c</sup>Cormack & Ruge (1994) they showed that a shallow-water primitive equation model using a semi-Lagrangian discretization of the pressure gradient terms like those in equation (19) produced large noisy errors in the absolute vorticity when compared to a model that conserves it. This is consistent with our findings here and we expect that they could alleviate their errors by using the form given in equation (20). This comes at the cost of reducing the temporal accuracy of the pressure gradient term from second to first order.

The ellipticity condition for the corrector equation constrains  $u_g$  to be constant across the equator and in an Eulerian scheme this stops cross-equatorial transport of  $\underline{u}_g$ . In the semi-Lagrangian scheme it is found that using  $V$  on the row next to the equator in the calculation of the departure point leads to significant numerical noise, which degrades the solution. Setting  $V$  on the row either side of the equator to zero removes this problem. This stops trajectories from crossing the equator and so stops cross-equatorial transport of  $\underline{u}_g$  in the semi-Lagrangian model just as in an Eulerian model. This is no a major restriction since we are still transferring mass correctly between the two hemispheres and the balanced wind field will adjust to fit with the mass field. Also the values of  $\underline{u}_g$  are very small near the equator and the cross-equatorial transport of them is an almost negligible term. It also found that



in calculating the departure point defining  $U$  at the equator to be the average of the  $U$  velocities either side of the equator gives a less noisy solution then using the actual  $U$  on the equator which has an undetermined rotational part.

## 2.D Ellipticity Enforcement

It is relatively easy to enforce inertial stability

$$\text{sign}(f)(f + \delta_\lambda v_g + u_g \tan \phi / a) > 0 \quad (21)$$

$$\text{sign}(f)(f - \delta_\phi u_g) > 0 \quad (22)$$

on  $\underline{u}_g$  provided that the second of these conditions is enforced first. We have multiplied each condition by the sign of  $f$  purely to make the condition positive in both hemispheres. A solution to (21) and (22) always exists provided that  $u_g \tan \phi / a$  is not significantly greater than  $f$ , which is the case only for non-physical flows by which time the solution is meaningless. Equation (21) also ensures that straight flow across the pole is inertially stable. These conditions are necessary but not sufficient for the full ellipticity condition for the correction equation (6) as shown by Shutts & Cullen (1987). To obtain a valid solution to the shallow-water semi-geostrophic equations the full condition must be enforced. Since the full condition is violated where  $q$  is small a conservative diffusion operator is applied where this occurs. This effectively mixes the low  $q$  values with the surrounding larger values and could be considered as a parametrization of horizontal mixing which occurs in areas of low inertial stability, as discussed in section 2. The diffusion equation for the corrections to  $q$  is given by

$$\Delta q = \frac{1}{a \cos \phi} \frac{\partial}{\partial \lambda} \left( \frac{C_\lambda}{a \cos \phi} \frac{\partial q}{\partial \lambda} \right) + \frac{1}{a} \frac{\partial}{\partial \phi} \left( C_\phi \frac{1}{a} \frac{\partial q}{\partial \phi} \right)$$

where the coefficients  $C_\lambda$  and  $C_\phi$  are tunable parameters. This diffusion should only be applied in the areas where it is likely the ellipticity condition will be violated, and so choose to specify the coefficients dependent on the current value of  $q$  relative to the value  $q$  would have if there was no flow, namely  $f^2$ . Noting that the maximum stable diffusion coefficients given by linear stability analysis are

$$C_\lambda^{max}(\phi) = \frac{1}{4} \frac{(a \Delta \lambda \cos \phi)^2}{\Delta t}$$



$$C_{\phi}^{max} = \frac{1}{4} \frac{(a\Delta\phi)^2}{\Delta t}$$

where the  $\lambda$ -direction coefficient depends on the latitude  $\phi$ , we define the  $q$  dependent coefficients at a point  $(\lambda, \phi)$  as

$$C_{\lambda}(\lambda, \phi) = \begin{cases} 0 & \text{if } q > \alpha f^2 \\ C_{\lambda}^{max}(\phi) \times (\alpha f^2 - q)/(f^2(\alpha - \beta)) & \text{if } \alpha f^2 \geq q \geq \beta f^2 \\ C_{\lambda}^{max}(\phi) & \text{otherwise} \end{cases}$$

and

$$C_{\phi}(\lambda, \phi) = \begin{cases} 0 & \text{if } q > \alpha f^2 \\ C_{\phi}^{max} \times (\alpha f^2 - q)/(f^2(\alpha - \beta)) & \text{if } \alpha f^2 \geq q \geq \beta f^2 \\ C_{\phi}^{max} & \text{otherwise} \end{cases}$$

where  $\alpha$  and  $\beta$  are parameters which control the switching on of the diffusion and the point below which the maximum stable value should be used. The choice of

$$\alpha = .25, \beta = .15$$

was used for all the cases considered in section 3. We now need to find the implied increments to the height field given by the diffusive correction  $\Delta q$  since the corresponding increments to  $\underline{u}_g$  can be found via the balance equations. The corrections are found by solving

$$g\nabla^2(\Delta h) = \Delta q \quad (23)$$

which is a simplified form of the full inversion equation to be solved to find the corrections to  $h$  implied by  $\Delta q$ . For the test problems solved in section 3 this procedure alleviated any problems with the formation of areas where the full ellipticity condition was violated.

## 2.E The Complete Procedure

The full predictor/corrector scheme can be summarised as follows

**Step 1**  $q$  dependent diffusion.

**Step 2** Prediction step.

The following steps are iterated  $n$  times;



**Step 3** Inertial stability enforced.

**Step 4** Corrector step.

## 2.F Convergence.

We noted in section 2 that as yet there is no analytic proof of existence and uniqueness of solutions to the shallow-water SG equations on the sphere. We also noted in section 2.B that we were unable to prove analytically that our simplified correction procedure converged to the same solution as the unapproximated correction procedure. Thus we need to ask the following two questions of our numerical method:

1. Does the solution obtained by this method converge as  $\Delta t$  tends to zero ?
2. Is the solution to which it converges the true solution of the original problem ?

We consider first the question of convergence. Suppose we are given data at time  $t_0$  then we need to prove that at any given fixed time  $t_1 > t_0$  the sequence  $H_n = h(\lambda, \phi, t_1; \Delta t_n)$  converges to a solution  $H$  as  $\Delta t_n$  tends to zero, for any fixed choice of  $\lambda$  and  $\phi$  on the sphere, where  $h(\lambda, \phi, t_1; \Delta t_n)$  is the solution to equations (2)-(5) at time  $t_1$  obtained by the predictor/corrector method described at the start of this section using a timestep  $\Delta t_n$ , and  $\Delta t_n$  is a strictly monotonic decreasing sequence which tends to zero as  $n$  tends to  $\infty$ . We need only show convergence of  $h$  as this determines the other fields via equations (2)-(5), provided that  $q \neq 0$  which we assume is true. Given that we do not know  $H$ , it is sufficient to prove convergence to show that the sequence is a Cauchy sequence, i.e. given  $\epsilon > 0$  there exists  $N$  such that  $\forall m, n > N$ ,

$$|H_n - H_m| < \epsilon$$

Since  $\Delta t_n \rightarrow 0$  as  $n \rightarrow \infty$  it is sufficient to show that,

$$|H_n - H_m| < M|\Delta t_n - \Delta t_m|$$

for some bounded constant  $M$ . We cannot obtain an analytic expression for  $h(\lambda, \phi, t_1; \Delta t_n)$ , however, we can demonstrate that for a fixed spatial resolution our numerical method



produces a sequence which appears to be a Cauchy sequence. We say appears to be because we cannot let  $\Delta t \rightarrow 0$  but simply run with many different timesteps and extrapolate. Showing convergence numerically of the numerical method at fixed resolution gives some indication that the procedure may converge for any resolution. We are unable at the moment to say more than this.

It then remains to show that this solution is the true solution. A necessary condition for the solution to be a solution of the SG equations is that  $R_{ew}$  and  $R_{ns}$  are zero for all time. We therefore need to show that as  $\Delta t \rightarrow 0$ , then  $R_{ew} \rightarrow 0$  and  $R_{ns} \rightarrow 0$  at every point in time in the domain. It is sufficient to show that  $R \rightarrow 0$  as  $\Delta t \rightarrow 0$  where

$$R = \int_{\Omega} \sum_{n=1}^{(t_1-t_0)/\Delta t} (|R_{ew}|_n + |R_{ns}|_n) \Delta t$$

and the domain  $\Omega$  is taken to be the sphere.  $R$  is simply the integral of the timestep-weighted absolute values of the residuals over the time interval.

We choose a fixed resolution of 192 by 129 points and take for our initial data real 500hpa fields valid at 20.00 GMT on the 4th June 1992 which we shall call time  $t_0$ . These fields were obtained by applying the initialisation method described in section 3.A. We choose time  $t_1$  to be 21.04 GMT on the same day and obtain the fields valid at this time via the numerical method with a particular choice of the timestep. We calculate  $E_{jk}$ ,  $M_{jk}$ ,  $E_{jk}^{\infty}$  and  $M_{jk}^{\infty}$  defined as follows,

$$E_{jk} = \frac{1}{N} \sum_{i=1}^N |h(\lambda_i, \phi_i, t_1, \Delta t_j) - h(\lambda_i, \phi_i, t_1, \Delta t_k)|$$

$$M_{jk} = E_{jk} / |\Delta t_j - \Delta t_k|$$

$$E_{jk}^{\infty} = \max_{1 \leq i \leq N} |h(\lambda_i, \phi_i, t_1, \Delta t_j) - h(\lambda_i, \phi_i, t_1, \Delta t_k)|$$

$$M_{jk}^{\infty} = E_{jk}^{\infty} / |\Delta t_j - \Delta t_k|$$

where  $i$  loops over all  $N$  points in the domain, and  $\Delta t_j$ ,  $\Delta t_k$  divide  $t_1 - t_0$  exactly.  $E_{jk}$  is the left-hand-side of the Cauchy inequality, except that it is the  $L_1$  mean over all points,  $E_{jk}^{\infty}$  is the largest value in the domain which typically occurs at the same point for all choices of  $\Delta t$ .  $M_{jk}$  and  $M_{jk}^{\infty}$  are the constants on the right-hand-side of the inequalities which we wish to bound to show convergence.  $\Delta t_1$  is chosen to be 1 minute and all timesteps in table 1 are in minutes.



j	$\Delta t_j$	$E_{1j}$	$M_{1j}$	$E_{1j}^\infty$	$M_{1j}^\infty$
2	2	$1.69287 \times 10^{-3}$	$1.69287 \times 10^{-3}$	$4.43717 \times 10^{-2}$	$4.43717 \times 10^{-2}$
3	4	$5.07752 \times 10^{-3}$	$1.69251 \times 10^{-3}$	0.13309	$4.43639 \times 10^{-2}$
4	8	$1.18414 \times 10^{-2}$	$1.69163 \times 10^{-3}$	0.31079	$4.43999 \times 10^{-2}$
5	16	$2.53515 \times 10^{-2}$	$1.69010 \times 10^{-3}$	0.66672	$4.44477 \times 10^{-2}$
6	32	$5.23244 \times 10^{-2}$	$1.68789 \times 10^{-3}$	1.38166	$4.45697 \times 10^{-2}$
7	64	$1.06575 \times 10^{-1}$	$1.69167 \times 10^{-3}$	2.82161	$4.47875 \times 10^{-2}$

Table 1:

We note that  $M = \sup(M_{1j})$  and  $M^\infty = \sup(M_{1j}^\infty)$  are bounded, in fact almost constant, and hence the solution is converging. Since we cannot run exhaustively all initial data with all timesteps we can never make a definitive statement about numerical convergence. However for all the cases we have run we have obtained results similar to those just shown.

For the same case and time period we also calculated

$$R_j = \sum_{i=1}^N \sum_{n=1}^{(t_1-t_g)/\Delta t_j} (|R_{ew}|_n + |R_{ns}|_n) \Delta t_j$$

where  $N$  is the number of grid-points in the domain. Assuming  $R \rightarrow 0$  as  $\Delta t \rightarrow 0$  then we can write

$$R = c\Delta t^n$$

for some constants  $c$  and  $n > 0$ . We wish to calculate  $c$  and  $n$  for this case. Taking timesteps in minutes we have that for  $\Delta t = 1$ ,  $c = R_1$  since

$$R_j = c\Delta t_j^n$$

and using this value for  $c$  we can calculate  $n$  for the other values of  $j$ , see table 2. These results show that  $R \rightarrow 0$  as  $\Delta t \rightarrow 0$  and so we believe that the solution of the semi-geostrophic equations is well defined and that the numerical method is converging to it. Again we cannot make a definite statement about convergence to the true solution, but for all the cases we have run we have found that  $R \rightarrow 0$  as  $\Delta t \rightarrow 0$ .



j	$\Delta t_j$	$R_j$	n
1	1	$2.02 \times 10^{-5}$	—
2	2	$7.97 \times 10^{-5}$	1.98
3	4	$3.11 \times 10^{-4}$	1.97
4	8	$1.19 \times 10^{-3}$	1.96
5	16	$4.29 \times 10^{-3}$	1.93
6	32	$1.36 \times 10^{-2}$	1.87
7	64	$2.89 \times 10^{-2}$	1.74

Table 2:



### 3 Computational Results

In this section computational results for several idealised and real data cases using the predictor/corrector method described in the last chapter are presented. The results are compared with those obtained from a C-grid primitive equation model, the semi-Lagrangian model of Bates et al. (1990). The only major difference in the implementation of the semi-Lagrangian scheme in the PE model is that the semi-Lagrangian form of the mass equation is used not the flux form used in the SG model. This means that the PE model does not explicitly conserve mass, although deviations from the initial global mean value are very small. Before presenting the results it is necessary to explain how initial data is obtained for both models, as initialising the SG model, particularly with real data, requires some care.

#### 3.A Data Initialisation

The shallow-water SG model requires consistent initial fields of  $h$ ,  $\underline{u}_g$  and  $\underline{u}$ . Given an initial height field, providing it is inertially stable and  $q$  is not zero, then all the other fields could be obtained directly from the SG equations after having calculated the initial values of  $\partial h/\partial t$ , and hence  $\partial \underline{u}_g/\partial t$ , by solving an elliptic equation for  $\partial h/\partial t$ . However the initial height field may not satisfy these constraints, as typically happens when using 500 hpa height fields from operational forecast models. This can occur in areas where geostrophic balance is inappropriate, such as low latitudes and areas of strong curvature, and also where the initial height field contains unbalanced motions. Many idealised problems used to test the shallow-water equations also suffer from the same failing, for example the problem of McDonald and Bates described in section 3.B.1 is inertially unstable near the equator, and the Rossby-Haurwitz wave problem, section 3.B.2, has areas of negative  $q$ . The direct method cannot be used to find the other fields when the initial height field does not satisfy the inertial stability constraints. To overcome this problem the following initialisation procedure is used in the SG model.



*Initialisation stage 1:* Take the initial height field and perform  $k$  iterations of the correction step from the predictor/corrector method but updating only the balanced velocity field  $\underline{u}_g$ . This gradually fits  $\underline{u}_g$  to the height field where possible. In areas where the balanced velocity field thus calculated violates the inertial stability conditions the constraints prevent the balanced wind field from fitting the height field exactly. The procedure can be summarized as

iterate  $k$  times

**Step 1** Corrector step. Updating  $\underline{u}_g$  only.

**Step 2** Inertial stability enforced.

*Initialisation stage 2:* Taking the fields from the end of the first stage as input, the correction step procedure is applied again but now allowing  $h$  is allowed to be updated as well. In areas where a valid solution could have been found by the direct method, the first stage of the initialisation should have also found that solution provided that  $k$  was large enough. In areas where a valid solution could not have been found a residual still exists and the second stage of the initialisation removes this residual whilst trying to minimize the affect on the solution in the other areas. The procedure is

iterate  $l$  times

**Step 1** Corrector step. Updating  $\underline{u}_g$  and  $h$ .

**Step 2** Inertial stability enforced.

The initial values of  $\underline{u}$  are defined to be equal to the balanced velocity obtained at the end of the second stage of the initialisation. In principle  $\underline{u}$  could be calculated exactly from equations (2) and (3) after first calculating  $\partial h / \partial t$  and  $\partial \underline{u}_g / \partial t$ , but in practice setting the initial values equal to the balanced velocity has been found to be sufficient.

The only serious problem with this initialisation procedure was found when trying to initialise the model with a uniform zonal flow. In this case the procedure successfully initialised the flow in mid to high latitudes but was very poor at



initialising in low latitudes. This is because the rate of convergence of the initialisation procedure when  $h$  updates are not allowed is proportional to  $f$ , and hence the number of iterations needed to obtain the solution is proportional to  $f^{-1}$  and near the equator tends to infinity. This problem is easily overcome by setting the uniform zonal flow directly since the height field satisfies the conditions required to use the direct method. In problems, such as the Rossby-Haurwitz problem, where a perturbation is applied to a uniform zonal flow we use the initialisation procedure after first setting the balanced velocities to satisfy the uniform zonal flow part of the initial data.

For all the problems considered in this section typical numbers used in the initialisation procedure are, 60 iterations of the first stage of the initialisation procedure and 10 iterations of the second stage. The most important thing to achieve is to fit the balanced wind field to the height field wherever possible and experiments show this to be achieved after 60 iterations. Only a few iterations of the second stage are required to remove the initial residuals to machine precision.

Primitive equation models are susceptible to gravity waves which are a solution not supported by the SG model. For many problems gravity waves can be generated by imbalances in the initial data, and appear as noise in the solution, which can lead to difficulty in interpreting the underlying solution to the problem. Two approaches are frequently used to overcome this problem. The first is to add a damping operator to the equations to suppress the gravity wave noise which has the disadvantage of introducing some smoothing into the underlying solution. The second approach is to use an initialisation scheme to remove the initial imbalances. This second approach is generally successful for some time period into the forecast, after which gravity wave noise can appear because of imbalances generated by forcing functions. For the unforced shallow-water equations there are very few imbalances generated by the numerical procedure, and a successful application of an initialisation procedure is usually sufficient to suppress the gravity waves for the whole forecast period in which we are interested, typically upto 10 days ahead. The digital filter initialisation procedure of Lynch & Huang (1992) was used to initialise the PE model in all the simulations that follow. For the idealised data cases, where



the initial wind fields are basically geostrophic, the initialisation procedure has little impact and both PE and SG models run from very similar initial data. For the real 500 hpa data the different initialisation procedures can lead to some significant differences between the two starting states. In all the experiments that follow a resolution of  $192 \times 129$  points was used and the timestep was 1800 seconds.

### 3.B Idealised Data

#### 3.B.1 McDonald-Bates 1989 Problem

This problem was posed in McDonald & Bates (1989) and is defined by setting the initial height field

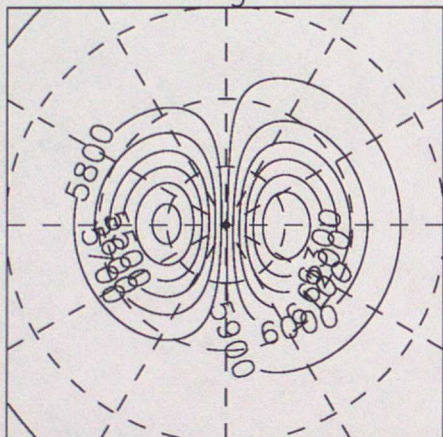
$$h(\lambda, \phi) = \bar{h} + \frac{af\bar{v}\sin^2\phi\sin\lambda}{g}$$

where  $\bar{h}$  and  $\bar{v}$  are fixed constants taken as  $\bar{h} = 57680/g$  metres and  $\bar{v} = 20ms^{-1}$ . This data represents a high/low system in each hemisphere which forces a flow of  $\bar{v}$  metres per second across the pole. The balanced wind field  $\underline{u}_g$  and the full wind field  $\underline{u}$  were then set via the initialisation procedure described in section 3.A, since the initial balanced velocities set directly using the balance equations are inertially unstable across the equator. The initialisation procedure removes this instability whilst having negligible impact on the initial data elsewhere on the sphere. Figure 2a shows the initial height field obtained in the northern hemisphere. Since the data is identical in the southern hemisphere, except that the high/low pair are rotated through 180 degrees of longitude charts are only shown for the northern one.

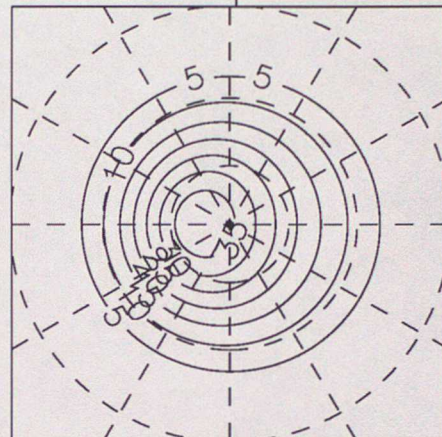
Figure 2 shows the height field after 5 days integration of the SG model and it is noticeably smooth and noise free. This can be further verified by looking at the  $q$  field after 5 days, figure 2d in which any noise would be more obvious since it is highly differentiated quantity. Comparing the height field after 5 days with the initial height field, we note that the high has gained height whilst the low is less intense. This differs from the solution obtained with the PE model, see figure 3a, where the low has weakened by a similar amount, 110m compared to 118m, but the high has declined by 110m instead of building slightly. The solution obtained by the PE model is similar to that shown in citeasnounmcba89 and Bates et al. (1990). The positions of the centres of the high and low agree quite well with the high very close



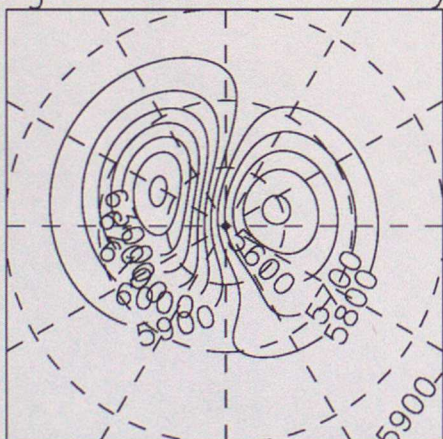
a) SG Model. MB89 Data  
Initial Height Field.



b) SG Model. MB89 Data  
Initial  $q$  Field.



c) SG Model. MB89 Data  
Height Field after 5 days.



d) SG Model. MB89 Data  
 $q$  Field after 5 days.

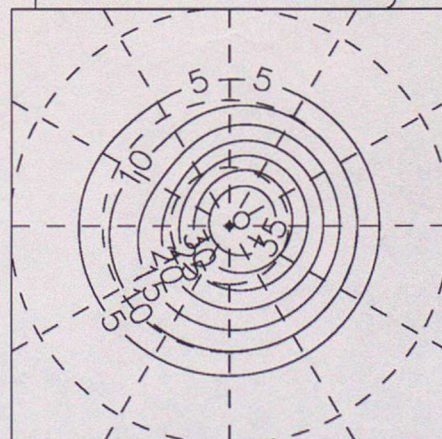
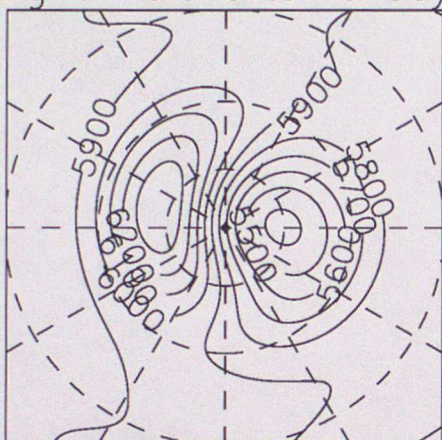


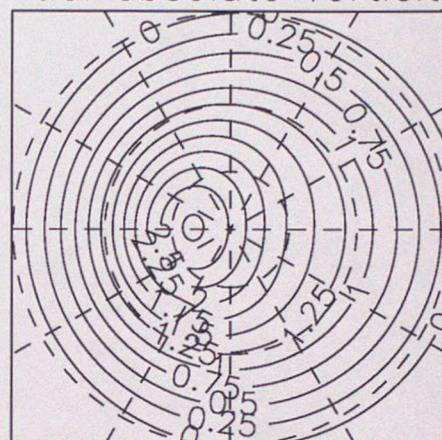
Figure 2: Contour intervals: Height field  $100m$ ,  $q$  field  $5 \times 10^{-13}$ .



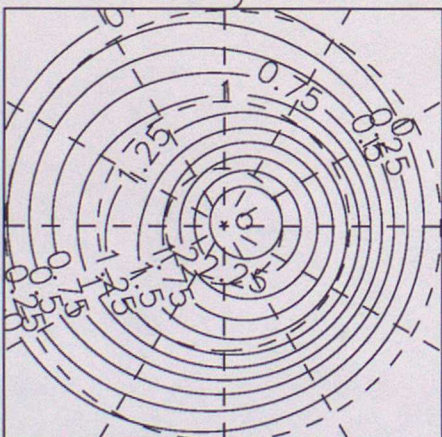
a) PE Model. MB89 Data  
Height Field after 5 days.



b) PE Model. MB89 Data  
Initial absolute vorticity.



c) PE Model. MB89 Data  
absolute vorticity after 5 days.



d) SG Model. MB89 Data  
absolute vorticity after 5 days.

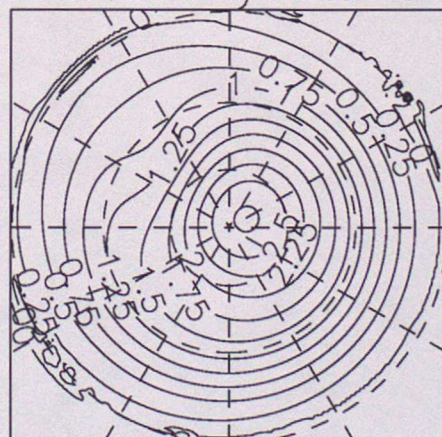


Figure 3: Contour intervals: Height field 100m, absolute vorticity field  $2.5 \times 10^{-7}$ .



to the same location, whilst the low in the SG model is approximately 7 degrees east of the PE centre. Since the solution is rotating clockwise this implies that the low in the SG model is rotating at approximately 1 degree per day slower than the PE low. The low in the SG model is more circular than the PE solution which shows a south-west to north-east slant. The SG solution being more symmetric than the PE solution was also found by Snyder et al. (1991) in their simulations of baroclinic waves on an  $f$ -plane. Apart from this difference the shape of the features is broadly similar. Figures 3c and 3d show the absolute vorticity after 5 days for the PE model and SG models respectively. It is immediately apparent that there is large ridging in the contours in the SG model, under and ahead of the high centre. This is also present in the PE model but much weaker. This ridging represents the presence of low absolute vorticity fluid near the high centre and is consistent with the maintenance of the high centre at its original value. Whitaker & Snyder (1993) have shown that for evolving baroclinic waves on the sphere the solution after 5 days is for highs and lows of approximately equal depth relative to the mean value. This is consistent with the result obtained here for the PE simulation of this barotropic problem. They also show that compared to the  $f$ -plane solution the PE solution has weaker lows and stronger highs. The  $f$ -plane SG solution for evolving baroclinic waves produces highs and lows of equal intensity whilst the PE solution produces deeper lows and weaker highs, see Snyder et al. (1991). Since the spherical geometry impacts should apply equally to SG and PE solutions this suggests that the SG solution for baroclinic waves on the sphere should have stronger highs than lows. This would agree with the SG solution shown here for the barotropic problem of McDonald and Bates.

### 3.B.2 The Rossby-Haurwitz Problem

Known solutions to the shallow-water primitive equations on the sphere are uncommon, with the most well-known being the Rossby-Haurwitz wave, see Haurwitz (1940). This wave will propagate from east to west at a known angular velocity without changing shape, if the equations are non-divergent. However, for the shallow-water equations with a free surface this is not the case. The propaga-



tion speed is reduced, the shape is no longer unchanged, and the wave is unstable for wave-numbers greater than 5, Hoskins (1973). This problem is still a standard test problem for the primitive shallow-water equations on the sphere and has been studied by many authors, for example, (Phillips 1959, Cullen 1974, Doron, Hollingsworth, Hoskins & Simmons 1974), and forms part of the NCAR test set for the shallow-water equations, Williamson, Drake, Hack, Jakob & Swarztrauber (1992). The problem is determined by four parameters; a scale height, the wave number, a parameter  $\omega$  which sets an underlying zonal wind field from west to east, and a parameter  $K$  which controls the amplitude of the wave. Complete details can be found in Phillips (1959). The standard problem used is wave-number 4 with  $\omega = k = 7.848 \times 10^{-6}$  and we would like to use this a test problem for the SG model. However, this standard problem has areas of negative absolute vorticity in the initial data. In fact no true Rossby-Haurwitz wave can be used as the initial conditions for the SG model because the data requires that a non-zero height gradient exists along the equator, see figure 5a for the Rossby-Haurwitz wave initial height data for the parameters; wave number 4,  $\omega = 7.848 \times 10^{-7}$ ,  $K = 7.848 \times 10^{-7}$  and a scale height,  $\phi_0 = 5500g$ . For small values of  $\omega$  and  $K$  the initialisation procedure of the SG model can be used without affecting the initial data extensively, the initialised height field for the parameters just given is shown in figure 4a. The SG model was run from this initialised field and the PE model from the analytic initial data. Running the PE model from the initialised field used as the starting field for the SG model produces a solution almost identical to that obtained by running the PE model from the analytic initial data. Figure 4b shows the height field from the SG model after 5 days. The field is largely unaltered with the axes of the troughs and ridges showing a slight westwards tilt. A similar result is gained for the primitive equations run from the true initial data, figure 5b. The main difference between the two solutions is the distance the wave has propagated to the west. In the SG model the wave has propagated approximately 60 degrees whilst in the PE model it has propagated approximately 96 degrees. The theoretical distance the wave should have propagated in a non-divergent primitive equation model is 101 degrees for the parameters chosen here. To understand this propagation behaviour a linearised



analysis of the non-divergent SG equations for travelling waves is performed following Shutts (1989), where in section 3.1 in his paper he performs the analysis for the planetary semi-geostrophic equations. The linearised non-divergent SG equations are,

$$\frac{\partial u_g}{\partial t} - 2\Omega v \sin\phi = \frac{-1}{a \cos\phi} \frac{\partial \Phi}{\partial \lambda} \quad (24)$$

$$\frac{\partial v_g}{\partial t} + 2\Omega u \sin\phi = \frac{-1}{a} \frac{\partial \Phi}{\partial \phi} \quad (25)$$

$$\frac{1}{\cos\phi} \left[ \frac{\partial u}{\partial \lambda} + \frac{\partial v \cos\phi}{\partial \phi} \right] = 0 \quad (26)$$

$$u_g \sin\phi = -\frac{1}{2\Omega a} \frac{\partial \Phi}{\partial \phi} \quad (27)$$

$$v_g \sin\phi = \frac{1}{2\Omega a \cos\phi} \frac{\partial \Phi}{\partial \lambda} \quad (28)$$

where  $\Phi = gh$ . Equations (24) and (25) can be used to give expressions for  $u$  and  $v$  in terms of  $\Phi$  using equations (27) and (28) to substitute for  $u_g$  and  $v_g$ . Substituting these expressions for  $u$  and  $v$  into equation (26) gives a partial differential equation for  $\Phi$ . Introducing the new variable

$$\mu = \sin\phi$$

and assuming that  $\Phi$  is a travelling wave of form

$$\Phi = G_m(\mu) e^{i(m\lambda - \sigma t)}$$

then the partial differential equation for  $\Phi$  is

$$\frac{(1 - \mu^2)}{\mu^2} \frac{\partial^2 G_m}{\partial \mu^2} - \frac{2}{\mu^3} \frac{\partial G_m}{\partial \mu} + \left( \frac{m\alpha_m}{\mu^2} - \frac{m^2}{\mu^2(1 - \mu^2)} \right) G_m = 0 \quad (29)$$

where

$$\alpha_m = -\frac{2\Omega}{\sigma}$$

This is the same equation as derived by Shutts, except for the factor of  $\mu^2$  in the denominator and a different  $\alpha_m$ . The  $\alpha_m$  we have derived here is identical to that derived for the primitive equations by Shutts, and hence for linearised non-divergent flow waves that can be completely represented by both SG and PE models should propagate with the same velocity. We note that the planetary semi-geostrophic equations have propagation speeds which are in excess of those for the SG and



primitive equations, as shown by Shutts. The equal propagation speeds for the SG and PE equation sets on an  $f$ -plane can be seen in the integrations of Whitaker (1993). However, as noted earlier, the Rossby-Haurwitz wave cannot be represented by the SG equations at the equator since it is inertially unstable. In creating the initial conditions for the SG model we have insisted that the data is inertially stable and this imposes a particular functional form on the solution at the equator. The inertial stability condition in the  $\phi$  direction is

$$\text{sign}(f) \left( \frac{1}{a} \frac{\partial}{\partial \phi} \left( \frac{g}{af} \frac{\partial h}{\partial \phi} \right) + f \right) > 0$$

Since  $f \rightarrow 0$  as  $\phi \rightarrow 0$  then the other term must also tend to zero to satisfy the condition. Let  $\psi$  be a function that tends to zero as  $\phi$  tends to zero and approximate  $f$  by  $\phi$  since near  $\phi = 0$   $\sin \phi \approx \phi$ , then

$$\frac{\partial}{\partial \phi} \left( \frac{1}{\phi} \frac{\partial h}{\partial \phi} \right) = \psi$$

Integrating twice with respect to  $\phi$  gives

$$h = \int \phi \left[ \int \psi d\phi \right] d\phi + c(\lambda)\phi^2 + d(\lambda)$$

and substituting this into the inertial stability condition in the  $\lambda$  direction at  $\phi = 0$  gives  $d(\lambda) = \text{constant}$ . Similarly substituting into the full ellipticity condition on  $q$  at  $\phi = 0$  implies that  $c(\lambda) = \text{constant}$ . Evaluating the integrals for the function  $\psi$  is not possible so instead we define

$$\mu = \int \phi \left[ \int \psi d\phi \right] d\phi$$

and note that  $\mu$  can be written in the general form

$$\mu = \phi^r p(\lambda, \phi)$$

for some power  $r$  and function  $p$ . Substituting this expression into the inertial stability condition in the  $\phi$  direction to determine the restrictions on  $r$  and  $p$  gives

$$r(r-2)\phi^{r-3}p + (2r-1)\phi^{r-2}\frac{\partial p}{\partial \phi} + \phi^{r-1}\frac{\partial^2 p}{\partial \phi^2}$$

which must tend to zero as  $\phi$  tends to zero. This is satisfied if  $r = 3 + \delta$  for some  $\delta > 0$  and  $p$  is a function with continuous second derivatives. Hence the general form of the solution at  $\phi = 0$  must satisfy

$$\Phi = d + c\phi^2 + \phi^{3+\delta}p(\lambda, \phi)$$



for some function  $p \in C^2$  and  $\delta > 0$ . Substituting the following expression for  $\Phi$

$$\Phi = \mu^{3+\delta} G_m(\mu) e^{i(m\lambda - \sigma t)}$$

since this satisfies the stability conditions and taking  $\delta = 0$  gives

$$\mu(1 - \mu^2) \frac{\partial^2 G_m}{\partial \mu^2} + (4 - 6\mu^2) \frac{\partial G_m}{\partial \mu} + \left( \mu m \alpha_m - 6\mu - \frac{m^2 \mu}{(1 - \mu^2)} \right) G_m = 0 \quad (30)$$

which can be compared with equation (29) which was obtained with the original substitution for  $\Phi$ . This is a generalised eigenvalue problem for  $\alpha_m$  and solutions were obtained by solving the discrete version obtained by applying centred finite-differences to the derivative terms in equation (30). For wave-number  $m = 4$  and using 129 points to discretise the interval all the eigenvalues are positive with the gravest mode corresponding to

$$\sigma \approx -\frac{4}{15}\Omega$$

which compares with the primitive equation gravest mode

$$\sigma = -\frac{2}{5}\Omega$$

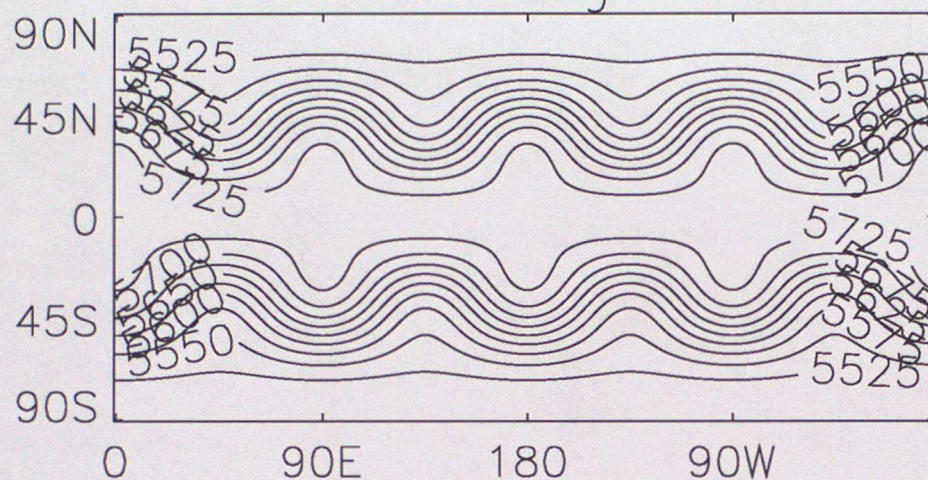
Hence the propagation speed of the wave in the SG model should be two-thirds of that of the wave in the primitive equation model. For the parameters chosen for the numerical experiment the wave in the SG model would have propagated 62 degrees in a non-divergent atmosphere, and this is in very good agreement with the 60 degrees that it propagated in the numerical experiment.

### 3.C Real 500hpa Height Data

We now wish to consider the ability of the SG model to handle real initial data to see if it is capable of producing realistic large scale evolution on the whole sphere. We take as our initial field the 500 hpa height field from an operational forecast model. Once again we do not have an analytic solution for this problem; however we wish to see if the evolution of the features found in the initial data is physically realistic. Since there is no external forcing in this problem, it is essentially more useful as a test of the numerical scheme than as a validation of the equations. However it allows us to review the behaviour of the equations in a more realistic environment than previously considered. In the simulation we expect that the motions



a) SG Model. Rossby–Haurwitz Data  
Initialized Height Field.



b) SG Model. Rossby–Haurwitz Data  
Height Field after 5 days.

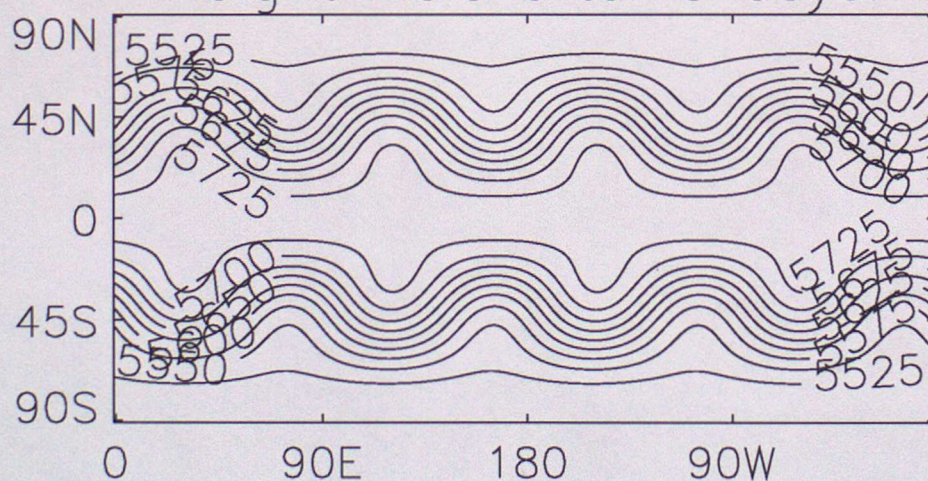
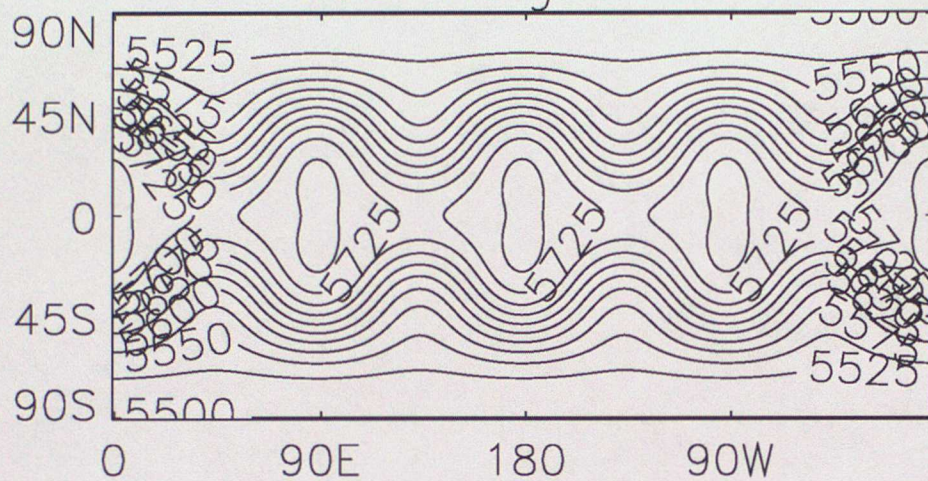


Figure 4: Contour interval 25m.



a) PE Model. Rossby–Haurwitz Data  
Initial Height Field.



b) PE Model. Rossby–Haurwitz Data  
Height Field after 5 days.

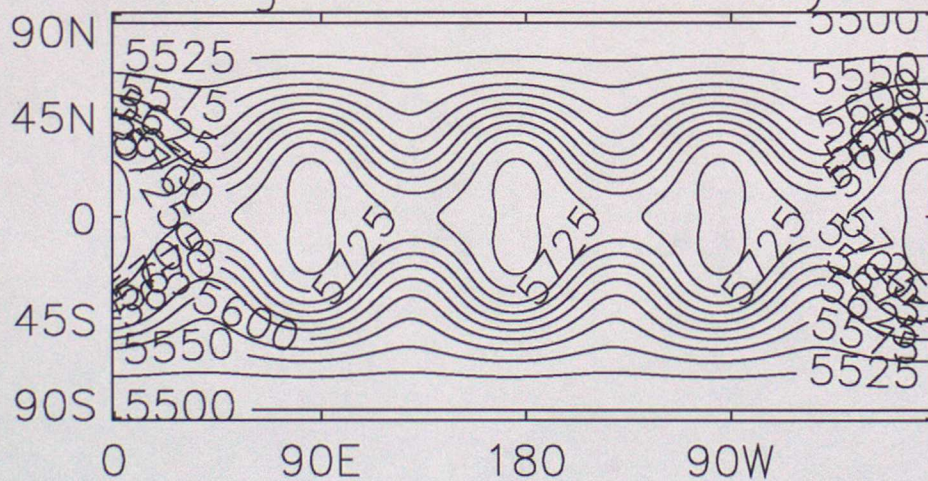


Figure 5: Contour interval 25m.



with the longest time and space scales should persist since they are better resolved, whilst the shorter scale motions should be lost. As a guide to the "correct" solution to the problem we take the solution from the primitive equation model. The initial data chosen are the 500hpa height field and wind fields from the 1st February 1991. This data contains a large blocking high over northern Europe and we expect that the shallow-water model should maintain this feature whilst it will probably lose the smaller scale lows which are visible in the southern hemisphere. The height field obtained after the SG model initialisation procedure is shown in figure 6a and the initialised PE height field is shown in figure 6b, with the differences plotted in figure 7a with contour interval 20m. The significant differences between the two fields occur in the areas of largest curvature, the eastern seaboard of the United States and in the low south of the tip of South America, where assuming the initial height field is in geostrophic balance produces an inertially unstable geostrophic wind field. The height field in the tropics is also flatter in the SG model than the PE model for the same reason. Figures 7b, 8a, 9a show the height field after 1, 3, and 10 days respectively of an integration of the SG model starting from this initial data. Looking at the first few days of the integration, it is noticeable how the smaller time-scale features are gradually disappearing whilst the main long time-scale feature, the blocking high over northern Europe, is largely unaltered. By day 5 this feature is the only significant one left and it persists throughout the ten days of the integration. This behaviour agrees with that expected and to further verify this we compare the results with those for the PE model for the same case. Figures 8b and 9b show the height field after 3 days and 10 days of the PE integration. The results of the two models after 3 days show very good agreement, better than that obtained for the idealised test cases. This suggests that the Lagrangian Rossby number, defined as

$$\frac{\left| \frac{Du}{Dt} \right|}{|f\bar{u}|}$$

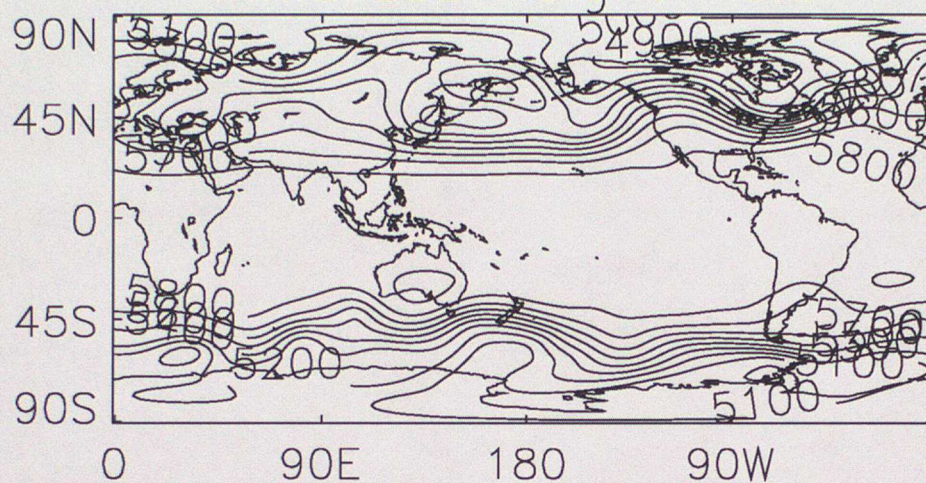
is small, much less than 1, for the flow, and hence that the geostrophic momentum approximation used to derive the SG equations from the PE equations holds, see Hoskins (1975). As noted in section 3.B.2, both models have the same phase speed for linearised non-divergent waves that are solutions of both equation sets. Since the waves in 500hpa flows are not of Rossby-Haurwitz type a better agreement in



pahse speeds is expected. The major areas of difference are in low latitudes where both models have formed high centres but in differing locations. This is not too surprising since the differences in the models are more pronounced in low latitudes where the PE model can support a wider variety of solutions than the SG model, and also since the differences in the initial conditions may be more significant than elsewhere. Comparing the features after 10 days, it is noticeable that the blocking high has been almost completely lost in the PE model whilst it is still prominent in the SG model. This again shows that the SG model has stronger highs than the PE model and hence persists them longer as was found for the McDonald-Bates idealised problem. This difference could be due to differences in evolution of the two models given that they were run from different initial conditions. However other real data cases have been run and they have shown similar characteristics.



a) SG Model. 500hpa Data from 1st Feb 1991  
Initialized Height Field.



b) PE Model. 500hpa Data from 1st Feb 1991  
Initialized Height Field.

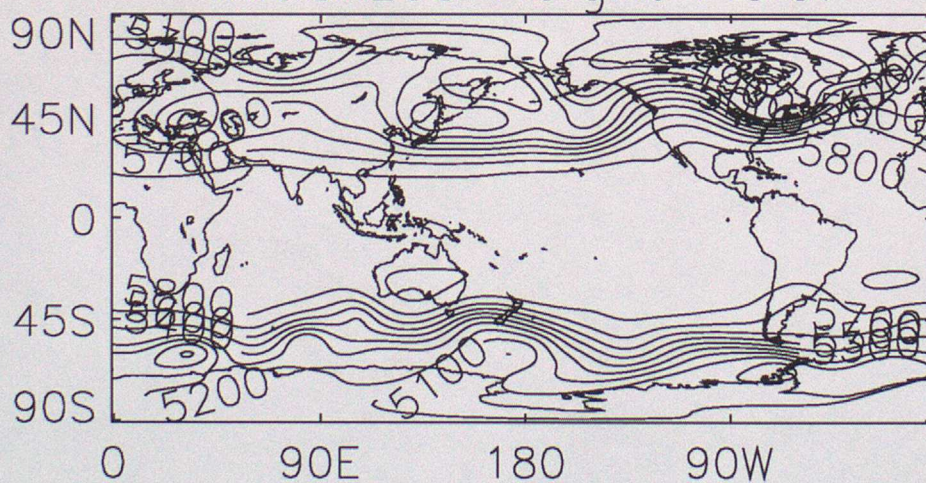
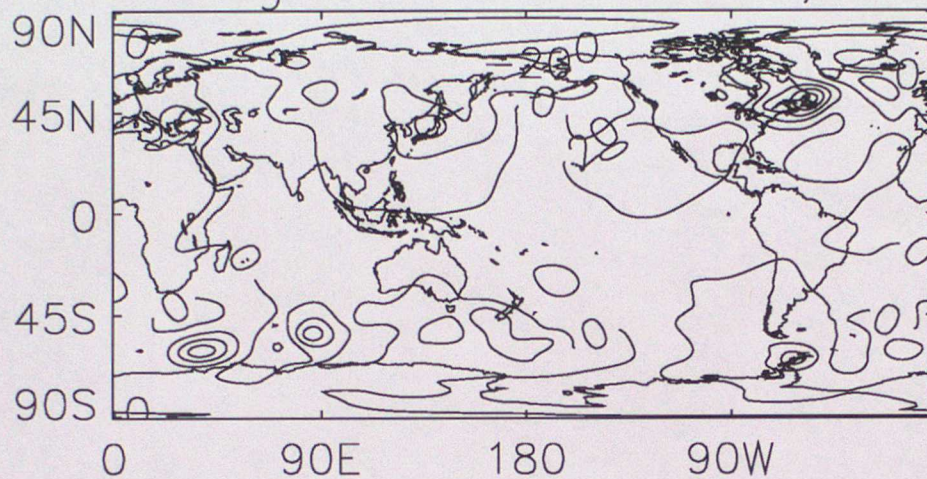


Figure 6: Contour interval 100m.



a) 500hpa Data from 1st Feb 1991  
Initial Height Field Difference, PE-SG.



b) QE Model. 500hpa Data from 1st Feb 1991  
Height Field after 1 day.

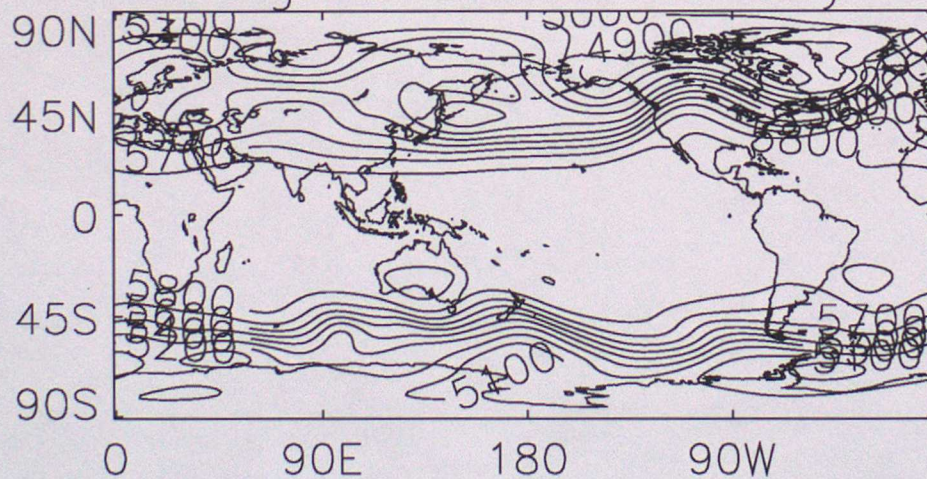
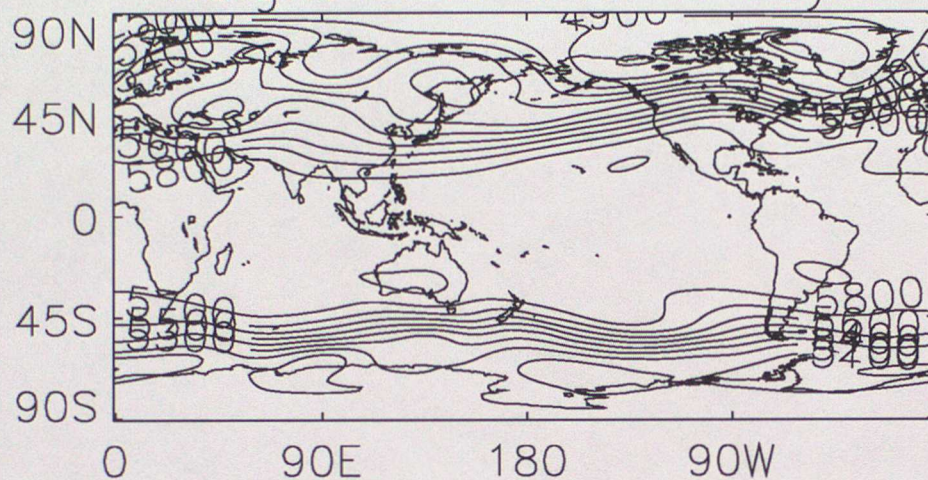


Figure 7: Contour intervals: Difference chart 20m, Height chart 100m.



a) SG Model. 500hpa Data from 1st Feb 1991  
Height Field after 3 days.



b) PE Model. 500hpa Data from 1st Feb 1991  
Height Field after 3 days.

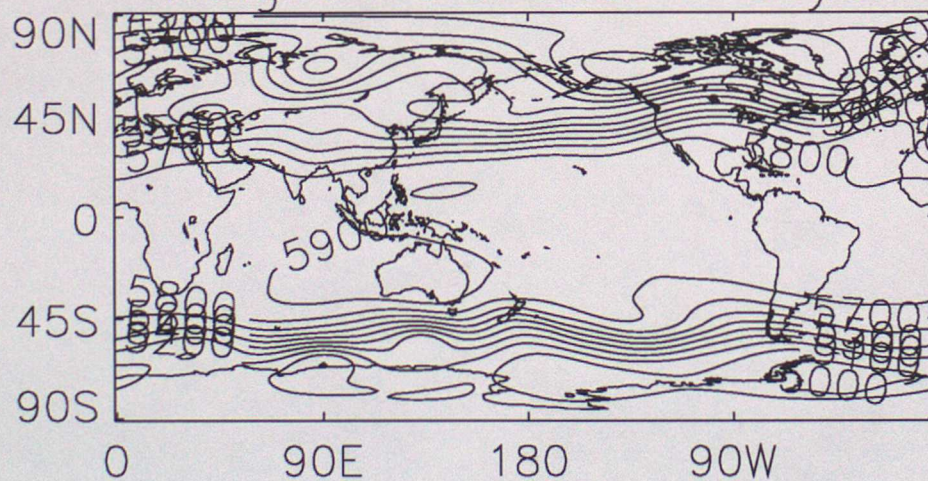
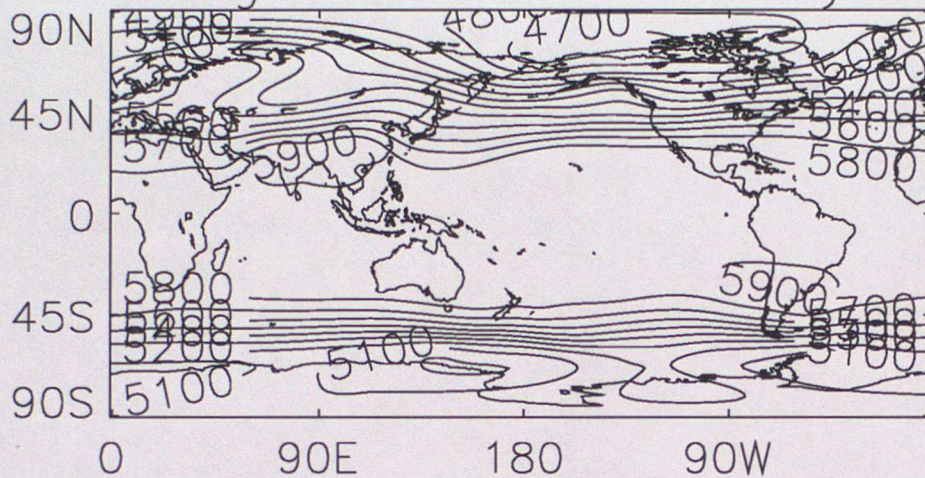


Figure 8: Contour interval 100m.



a) SG Model. 500hpa Data from 1st Feb 1991  
Height Field after 10 days.



b) PE Model. 500hpa Data from 1st Feb 1991  
Height Field after 10 days.

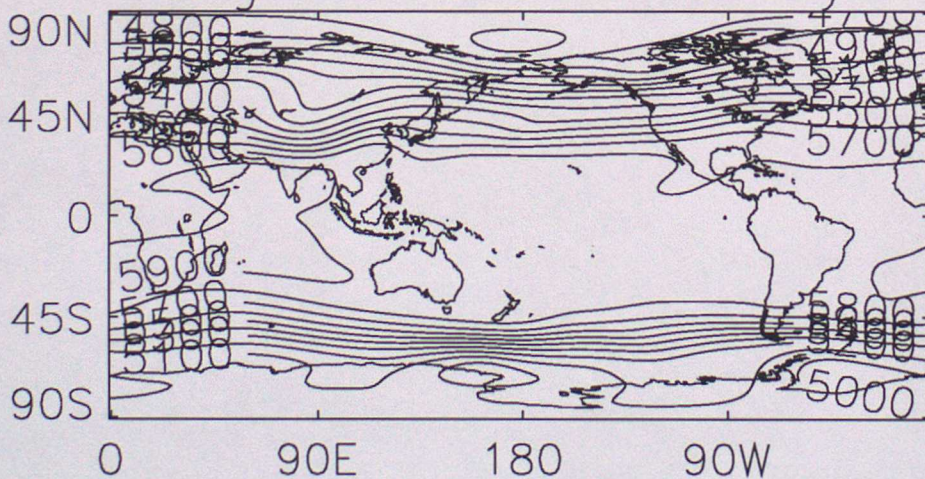


Figure 9: Contour interval 100m.



## 4 Conclusions

A semi-Lagrangian predictor/corrector method for solving the shallow-water semi-geostrophic equations on the sphere has been described and it has been shown to be stable and accurate for the test problems attempted here. It has been demonstrated, numerically, that for fixed spatial resolution the method appears to converge to a true solution of the semi-geostrophic equations as the timestep tends to zero. Convergence of the analytic equivalent of the numerical procedure converged to a unique solution is currently unproven; these numerical results suggest nevertheless that this solution is well-defined. In constructing the semi-Lagrangian predictor step failures of the model were observed in the vicinity of the poles and this was due to excessive noise being introduced in the  $q$  field. This noise is caused by the treatment of the pressure gradient terms on the C grid which introduce a significant lack of conservation in the geostrophic absolute vorticity. This non-conservation can be removed by altering the way the terms are treated but at the penalty of making them only first order accurate in time. This has implications for C grid semi-Lagrangian primitive equation models which will introduce a similar non-conservation into the absolute vorticity near the poles if they use the same formulation of the pressure gradient terms. This noise has been observed by Bates et al. (1994) when comparing a potential vorticity conserving and non-potential vorticity conserving primitive equation model.

The solutions obtained from the semi-geostrophic model are in broad agreement with those obtained from a primitive equation model for the test problem of McDonald & Bates (1989) and for a 500hpa real data case. The major difference between the solutions is that the semi-geostrophic model supports stronger high pressure areas and in the unforced problems considered here is seen in the SG model persisting the highs for longer than the PE model. This behaviour is consistent with that expected from the work of Snyder et al. (1991) and Whitaker & Snyder (1993). The semi-geostrophic model cannot represent a traditional Rossby-Haurwitz wave, although for a small amplitude Rossby-Haurwitz wave it is possible to run a simulation after first removing the areas of inertial instability. The resulting wave propagates much slower than the traditional Rossby-Haurwitz wave but in good



agreement with the propagation speed expected from a linear analysis.

The numerical algorithm could be extended to three-dimensions but will require some care near the equator. In future work we hope to complete the extension and to look at semi-geostrophic simulation of more realistic problems, including coupling the dynamics to a sophisticated physics package. It remains to be seen if such three-dimensional simulations will provide any further significant insight into the atmosphere or our understanding of numerical models.

*Acknowledgements.* The author would like to acknowledge the help of Dr Mike Cullen, U.K. Met. Office, and Dr Mike Baines, University of Reading, with many aspects of this work. The author would also like to thank Dr Ray Bates, NASA Goddard, for supplying the semi-Lagrangian code.



## References

- Allen, J. S., Barth, J. A. & Newberger, P. A. 1990 , On intermediate models for barotropic continental shelf and slope field flows: Part 1, formulation and comparison of exact solutions, *J. Phys. Oceanogr.* **20**, 1949–1973.
- Barros, S. R. M. 1991 , Multigrid methods for two- and three-dimensional poisson-type equations on the sphere, *J. Comp. Phys.* **92**, 313–348.
- Bates, J. R., Li, Y., Brandt, A., M<sup>c</sup>Cormack, S. F. & Ruge, J. 1994 , A global barotropic primitive equation model based on the semi-lagrangian advection of potential vorticity, Submitted to *Q. J. R. Meteorol. Soc.*
- Bates, J. R., Semazzi, F. H. M., Higgins, R. W. & Barros, S. R. M. 1990 , Integration of the shallow water equations on the sphere using a semi-lagrangian scheme with a multigrid solver, *Mon. Weather Rev.* **118**, 1615–1627.
- Castelli, F., Bras, R. L. & Emanuel, K. A. 1993 , An analytic approach to the non-linear dynamics of moist frontogenesis, *J. Atmos. Sci.* **50**, 1504–1518.
- Charney, J. G., Fjortoft, R. & von Neumann, J. 1950 , Numerical integration of the barotropic vorticity equation, *Tellus* **2**, 237–254.
- Cullen, M. J. P. 1974 , Integrations of the primitive equations on a sphere using the finite element method, *Q. J. R. Meteorol. Soc.* **100**, 555–562.
- Cullen, M. J. P. 1989*a* , Implicit finite-difference method for modelling discontinuous atmospheric flows, *J. Comp. Phys.* **81**, 319–348.
- Cullen, M. J. P. 1989*b* , On the incorporation of atmospheric boundary layer effects into a balanced model, *Q. J. R. Meteorol. Soc.* **115**, 1109–1131.
- Cullen, M. J. P. & Purser, R. J. 1989 , Properties of the lagrangian semigeostrophic equations, *J. Atmos. Sci.* **46**, 2684–2697.
- Cullen, M. J. P., Chynoweth, S. & Purser, R. J. 1987 , On semi-geostrophic flow over synoptic scale topography, *Q. J. R. Meteorol. Soc.* **113**, 163–180.



- Davies, H. C., Schar, C. & Wernli, W. 1991 , The palette of fronts and cyclones within a baroclinic wave development, *J. Atmos. Sci.* **48**, 1666–1689.
- Doron, E., Hollingsworth, A., Hoskins, B. J. & Simmons, A. J. 1974 , A comparison of grid-point and spectral methods in a meteorological problem, *Q. J. R. Meteorol. Soc.* **100**, 371–383.
- Eliassen, A. 1948 , The quasi-static equations of motion, *Geofys. Publ.* **17**, No. 3.
- Gent, P. R. & McWilliams, J. C. 1983*a* , Consistent balanced models in bounded and periodic domains, *Dyn. Atmos. Oceans* **7**, 67–93.
- Gent, P. R. & McWilliams, J. C. 1983*b* , Regimes of validity for balanced models, *Dyn. Atmos. Oceans* **7**, 167–183.
- Haurwitz, B. 1940 , The motion of atmospheric disturbances on the spherical earth, *J. Marine Res.* **3**, 254–267.
- Holt, M. W. 1990 , Semi-geostrophic moist frontogenesis in a lagrangian model, *Dyn. Atmos. Oceans* **14**, 463–481.
- Holt, M. W. & Thorpe, A. J. 1991 , Localized forcing of slantwise motion at fronts, *Q. J. R. Meteorol. Soc.* **117**, 943–963.
- Hoskins, B. J. 1973 , Stability of the rossby-haurwitz wave, *Q. J. R. Meteorol. Soc.* **99**, 723–745.
- Hoskins, B. J. 1975 , The geostrophic momentum approximation and the semi-geostrophic equations, *J. Atmos. Sci.* **32**, 233–242.
- Hoskins, B. J. & Bretherton, F. P. 1972 , Atmospheric frontogenesis models: mathematical formulation and solution, *J. Atmos. Sci.* **29**, 11–37.
- Lynch, P. & Huang, X.-Y. 1992 , Initialisation of the hirlam model using a digital filter, *Mon. Weather Rev.* **120**, 1019–1034.
- Mawson, M. H. 1994 , The shallow-water semi-geostrophic equations on the sphere, Ph. D. Thesis, University of Reading.



- McDonald, A. & Bates, J. R. 1989 , Semi-lagrangian integration of a gridpoint shallow-water model on the sphere, *Mon. Weather Rev.* **117**, 130–137.
- McWilliams, J. C. & Gent, P. R. 1980 , Intermediate models of planetary circulations in the atmosphere and ocean, *J. Atmos. Sci.* **37**, 1657–1678.
- Phillips, N. A. 1959 , Numerical integration of the primitive equations on the sphere, *Mon. Weather Rev.* **87**, 333–345.
- Pierrehumbert, R. T. 1985 , Stratified semi-geostrophic flow over two-dimensional topography in an unbounded domain, *J. Atmos. Sci.* **42**, 523–526.
- Rodwell, M. J. & Hoskins, B. J. 1995 , A model of the asian summer monsoon. ii: Cross-equatorial flow and pv behaviour, to appear in *J. Atmos. Sci.*
- Salmon, R. 1985 , New equations for nearly geostrophic flow, *J. Fluid Mech.* **153**, 461–477.
- Shutts, G. J. 1989 , Planetary semi-geostrophic equations derived from hamilton's principle, *J. Fluid Mech.* **208**, 545–573.
- Shutts, G. J. & Cullen, M. J. P. 1987 , Parcel stability and its relation to semi-geostrophic theory, *J. Atmos. Sci.* **44**, 1318–1330.
- Snyder, C., Skamarock, W. C. & Rotunno, R. 1991 , A comparison of primitive equation and semi-geostrophic simulations of baroclinic waves, *J. Atmos. Sci.* **48**, 2179–2194.
- Van, J. P. & Raithby, G. D. 1984 , Enhancements to the simple method for predicting incompressible fluid flows, *Numer. Heat Transfer* **7**, 147–163.
- Wen, X. & Ingham, D. B. 1993 , A new method for accelerating the rate of convergence of simple-like algorithms, *Int. J. Num. Meth. Fluids* **17**, 385–400.
- Whitaker, J. S. 1993 , A comparison of primitive and balance equation simulations of baroclinic waves, *J. Atmos. Sci.* **50**, 1519–1530.
- Whitaker, J. S. & Snyder, C. 1993 , The effects of spherical geometry on the evolution of baroclinic waves, *J. Atmos. Sci.* **50**, 597–612.



- Williamson, D. L., Drake, J. B., Hack, J. J., Jakob, R. & Swarztrauber, P. N. 1992 , A standard test set for numerical approximations to the shallow-water equations in spherical geometry, *J. Comp. Phys.* **102**, 221–224.
- Wu, R. & Blumen, W. 1982 , An analysis of ekman boundary layer dynamics incorporating the geostrophic momentum approximation, *J. Atmos. Sci.* **39**, 1774–1782.
- Young, J. A. 1973 , A theory for isallobaric flow in the planetary boundary layer, *J. Atmos. Sci.* **30**, 1584–1592.



FORECASTING RESEARCH DIVISION SCIENTIFIC PAPERS  
(List valid 04/01/95)

This series of Forecasting Research Division (FR) Scientific Papers . will be papers from all three sections of the Forecasting Research Division i.e. Data Assimilation Research (DA), Numerical Modelling Research (NM), and Observations and Satellite Applications (OB) the latter being formerly known as Nowcasting (NS). This series succeeds the series of Short Range Forecasting Research /Met O 11 Scientific Notes.

1. THE UNIFIED FORECAST /CLIMATE MODEL .  
M.J.P. Cullen  
September 1991
2. Preparation for the use of Doppler wind lidar information  
in meteorological data assimilation systems  
A.C. Lorenc, R.J. Graham, I. Dharssi, B. Macpherson,  
N.B. Ingleby, R.W. Lunnon  
February 1992
3. Current developments in very short range weather  
forecasting.  
B.J. Conway  
March 1992
4. DIAGNOSIS OF VISIBILITY IN THE UK MET OFFICE MESOSCALE  
MODEL  
AND THE USE OF A VISIBILITY ANALYSIS TO CONSTRAIN INITIAL  
CONDITIONS  
S.P. Ballard, B.J. Wright, B.W. Golding  
April 1992
5. Radiative Properties of Water and Ice Clouds at  
Wavelengths  
Appropriate to the HIRS Instrument  
A.J. Baran and P.D. Watts  
2nd June 1992
6. Anatomy of the Canonical Transformation  
M.J. Sewell and I. Roulstone  
27 June 1992
7. Hamiltonian Structure of a Solution Strategy for the  
Semi-Geostrophic Equations  
I. Roulstone and J. Norbury  
29 June 1992
8. Assimilation of Satellite Data in models for energy  
and water cycle Research  
A.Lorenc  
July 1992



FORECASTING RESEARCH DIVISION SCIENTIFIC PAPERS

(As of 04/01/95)

9. The use of ERS-1 data in operational meteorology  
A.Lorenc, R.S.Bell, S.J.Foreman, M.W.Holt, D.Offiler  
C.D.Hall, D.L.Harrison, S.G.Smith  
August 1992
10. Bayesian quality control using multivariate normal  
distributions  
N.B. Ingleby and A. Lorenc  
July 1992
11. A NEW APPROACH TO SHALLOW FLOW OVER AN OBSTACLE  
I General Theory  
A.S. Broad, D. Porter and M.J. Sewell  
10 August 1992
12. A NEW APPROACH TO SHALLOW FLOW OVER AN OBSTACLE  
II Plane Flow over a Monotonic Mountain  
A.S. Broad, D. Porter and M.J. Sewell  
10 August 1992
13. A Balanced Ocean Model with Outcropping  
Paul Cloke and M.J.P.Cullen  
August 1992
14. OSCILLATIONS IN THE ATMOSPHERE'S ANGULAR MOMENTUM  
AND TORQUES ON THE EARTH'S BULGE  
M.J. Bell September 1992
15. Preliminary assessment and use of ERS-1 altimeter  
wave data  
S.J.Foreman, M W Holt and S Kelsall  
November 1992
16. NON-GAUSSIAN PROBABILITIES IN DATA ASSIMILATION  
AND QUALITY CONTROL DECISIONS  
Andrew C Lorenc  
November 1992
17. Precipitation estimation with AVHRR data: a review  
G.L. Liberti  
February 1993
18. REAL-TIME CORRECTION OF WEATHER RADAR DATA FOR THE  
EFFECTS OF BRIGHT BAND, RANGE AND OROGRAPHIC GROWTH  
M.Kitchen, R Brown and A G Davies  
July 1993
19. A Semi-Geostrophic Ocean Model with Outcropping  
Paul Cloke and M.J.P. Cullen  
August 25, 1993



FORECASTING RESEARCH DIVISION    SCIENTIFIC PAPERS

20. Families of Contact Transformations  
M.J. Sewell and I. Roulstone  
10 December 1993
21. Global Processing Of Satellite Sounding Radiances  
In A Numerical Weather Prediction System  
A.J. Gadd, B.R Barwell, S.J. Cox, and R.J. Renshaw  
January 1994
22. A Hamiltonian Formulation of the Quasi-Hydrostatic  
Equations.  
I .Roulstone and S.J. Brice  
5th April 1994
23. THE CORIOLIS FORCE IN GLOBAL ATMOSPHERIC MODELS  
I. THE NAVIER-STOKES EQUATION AND THE HYDROSTATIC  
PRIMITIVE EQUATIONS  
A.A. White, R.A. Bromley, and B.J. Hoskins  
April 1994
24. THE CORIOLIS FORCE IN GLOBAL ATMOSPHERIC MODELS  
II. DYNAMICALLY CONSISTENT QUASI-HYDROSTATIC EQUATIONS  
A.A. White, and R.A. Bromley  
April 1994
25. The 1D, Vertical, Version of the Proposed Semi-Implicit  
Integration Scheme for the Unified Model: Formulation  
and Test Results.  
S. Coulter and M.H. Mawson  
October 1994
26. Some issues in numerical methods for the next generation  
of NWP and climate models  
M.P.J. Cullen, T.Davies, M.H. Mawson, J.A. James,  
S. Coulter and A. Malcolm  
October 1994
27. A Comparison of two vertical grid staggerings  
M.J.P. Cullen and J.James  
August 1994
28. On the use of radiosonde humidity observations in  
midlatitude NWP  
A.C. Lorenc, D.Barker, R.S.Bell, B.Macpherson and  
A.J.Maycock
29. NEW SHALLOW FLOWS OVER AN OBSTACLE  
A.S. Broad, D. Porter and M.J. Sewell  
19 October 1994



FORECASTING RESEARCH DIVISION SCIENTIFIC PAPERS

30. A shallow-water semi-geostrophic model on the sphere  
M.H.Mawson  
January 1995